# Figure S1.

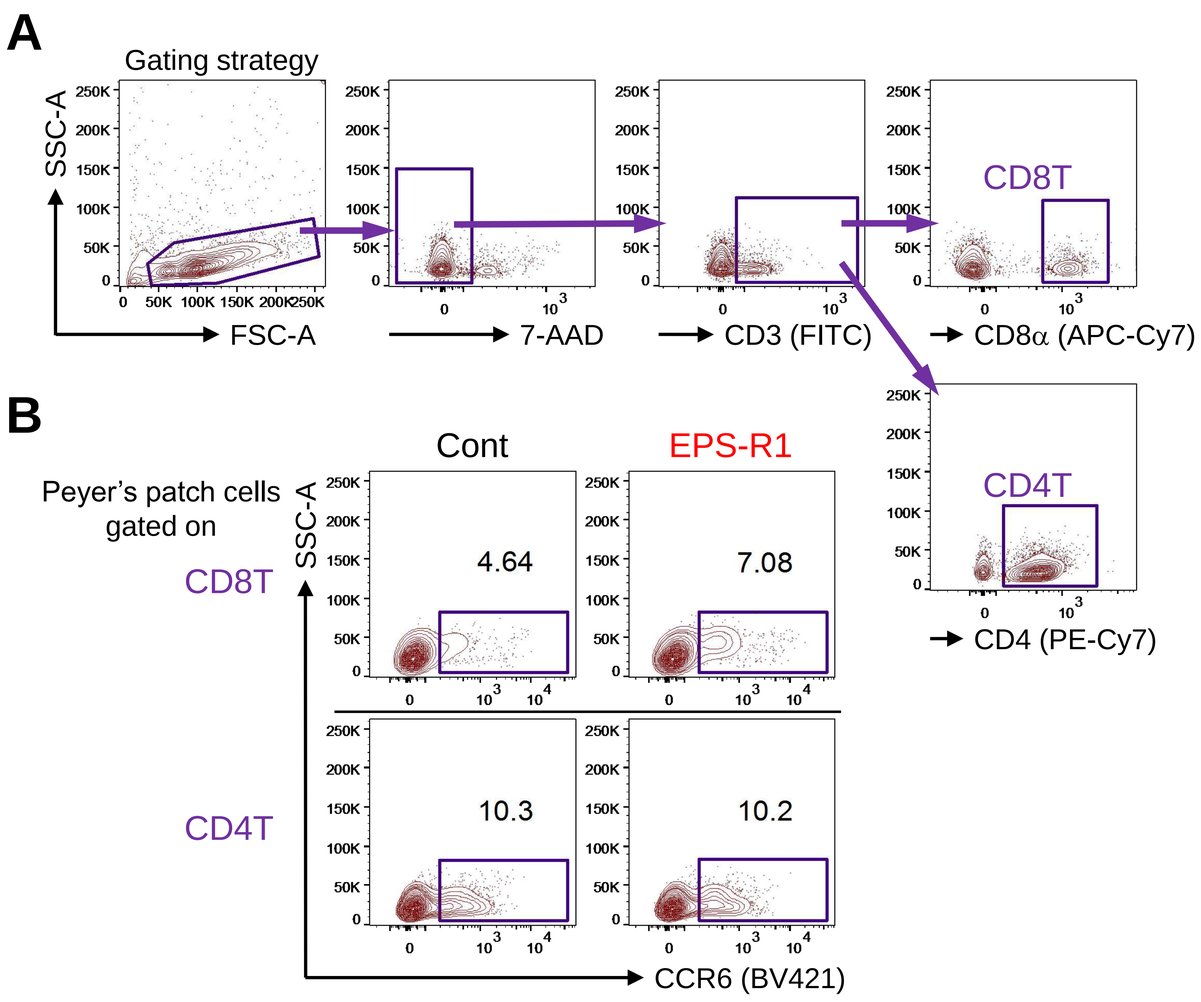
A
Gating strategy
SSC-A
FSC-A
7-AAD
CD3 (FITC)
CD8α (APC-Cy7)
CD8T
CD4T
CD4 (PE-Cy7)
B
Cont
EPS-R1
Peyer's patch cells gated on
CD8T
CD4T
4.64
7.08
10.3
10.2
CCR6 (BV421)


C
EPS-R1-ingested
jejunum
ileum

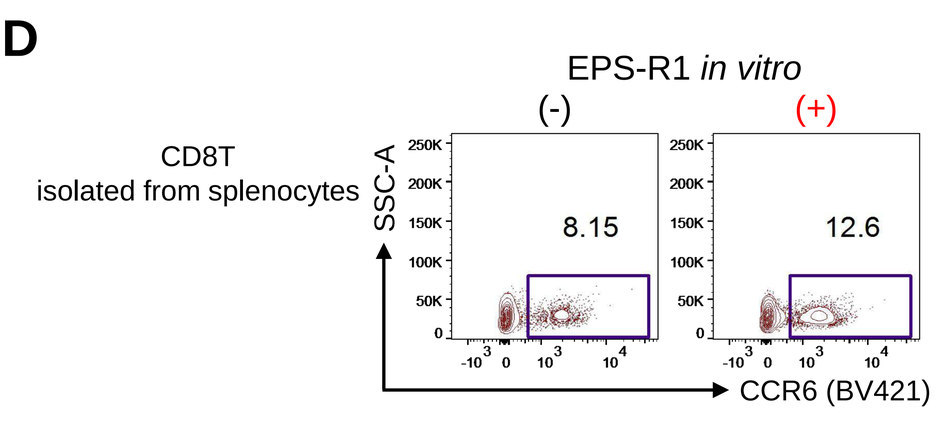
D
EPS-R1 in vitro
(-)
(+)
CD8T
isolated from splenocytes
SSC-A
8.15
12.6
CCR6 (BV421)

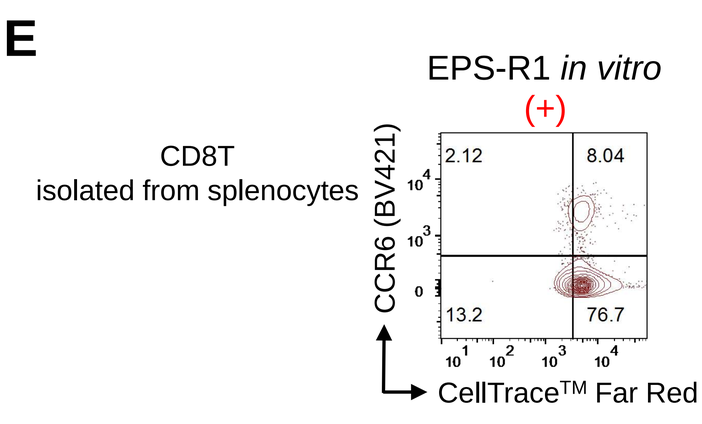
E
EPS-R1 in vitro
(+)
CD8T
isolated from splenocytes
CCR6 (BV421)
2.12
8.04
13.2
76.7
CellTrace™ Far Red

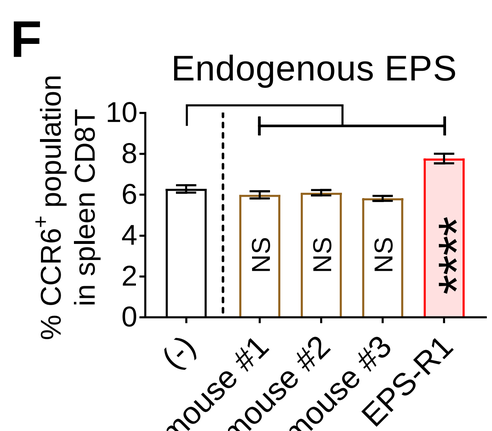
F
Endogenous EPS
% CCR6+ population in spleen CD8T
NS
NS
NS
****
(-)
EPS-mouse #1
EPS-mouse #2
EPS-mouse #3
EPS-R1

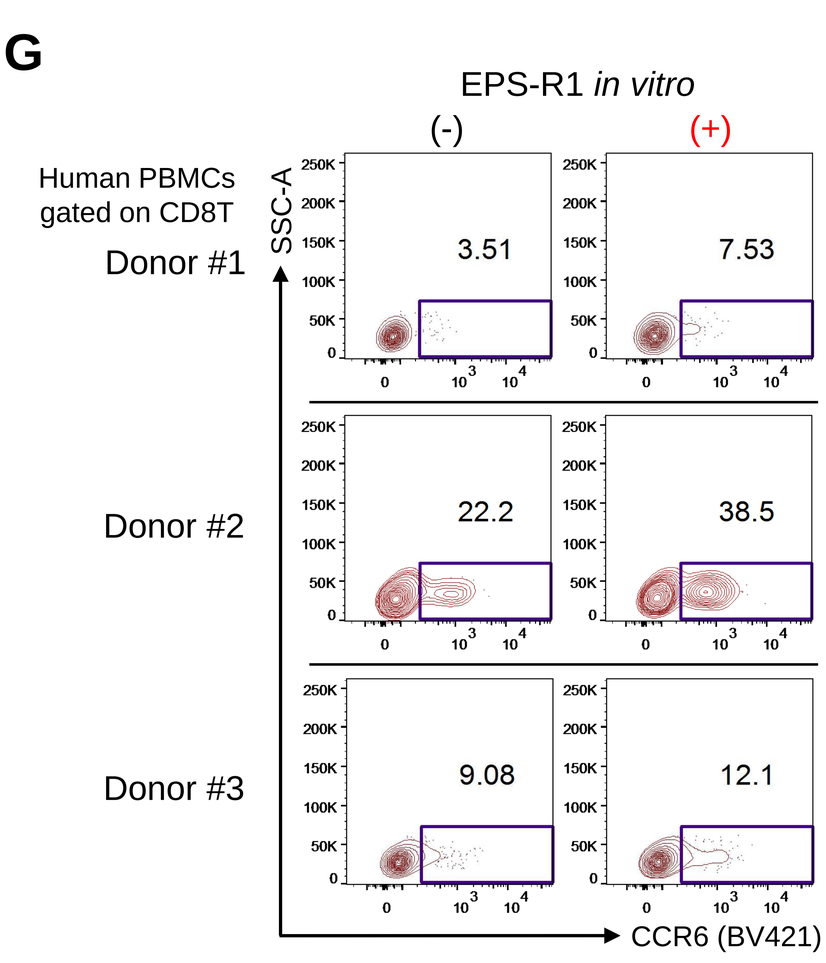
G
EPS-R1 in vitro
(-)
(+)
Human PBMCs gated on CD8T
Donor #1
Donor #2
Donor #3
SSC-A
3.51
7.53
22.2
38.5
9.08
12.1
CCR6 (BV421)

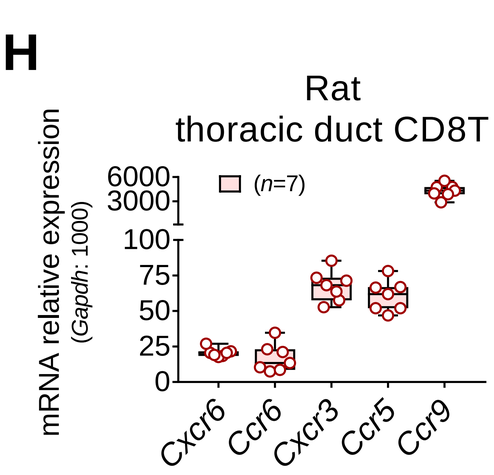
H
Rat
thoracic duct CD8T
mRNA relative expression
(Gapdh: 1000)
(n=7)
Cxcr6
Ccr6
Cxcr3
Ccr5
Ccr9

**Supplementary Figure S1. Representative profiles of flow cytometric analysis for CCR6 expression on $CD8^+$ T cells, chemokine receptor gene expression in rat thoracic duct $CD8^+$ T cells and histological analysis of intestines of EPS-R1-ingested mice.**

**A,** After dietary ingestion of EPS-R1 for 6 days, MNCs were prepared from Peyer's patches. CCR6 expression on $CD8^+$ and $CD4^+$ T cells was then analyzed using the indicated gate setting process by flow cytometry. **B,** Representative contour plots of CCR6 expression on $CD8^+$ and $CD4^+$ T cells from control mice and EPS-R1-ingested mice demonstrated in (A). **C,** Following dietary ingestion of EPS-R1 for 6 days, jejunum and ileum were obtained and examined by hematoxylin and eosin staining. Representative macroscopic tissue images (concatenated x40 images) and microscopic tissue images (x200) are presented in the top panels and the bottom panels respectively. Bar lengths are 1000 μm (in top panels) or 100 μm (in bottom panels). **D,** Representative contour plots of CCR6 expression on $CD8^+$ T cells isolated from splenic MNCs stimulated with or without EPS-R1 for 24 h *in vitro*. **E,** Representative contour plot of CellTrace™ analysis for the proliferation of $CD8^+$ T cells isolated from splenic MNCs 24 h after EPS-R1 stimulation *in vitro*. **F,** Splenocytes freshly prepared from BALB/c WT mice were stimulated with EPS-R1 or EPSs prepared from small intestinal contents of 3 mice for 24 h *in vitro*, and then the $CCR6^+$ population amongst $CD8^+$ T cells were examined by flow cytometry ($n$ = 8). The results are presented as mean ± SEM and statistical analysis was performed by one-way ANOVA with Dunnett correction. NS, not significant. ****$P$ < 0.0001. **G,** Representative contour plots of CCR6 expression on human $CD8^+$ T cells in PBMCs stimulated with or without EPS-R1 for 24 h *in vitro*. Results of 3 volunteers are presented. **H,** $CD8^+$ T cells were isolated from lymphocytes in the thoracic duct lymph of Wistar/ST rats, and gene expression of 5 chemokine receptors was examined by RT-qPCR methods. The results are presented as box plots with individual samples ($n$ = 7). Square gates (A, B, D and G) were set basing on the staining profile with isotype-matched control mAb, and quadra gate (E) was set basing on the staining profile of pre-culture control stained with CellTrace™ Far Red. % of gated $CCR6^+$ cells (B, D and G) or % in quadra gates (E) are presented in the panels.

FSC-A, forward scatter area; SSC-A, side scatter area; CD8(4)T, $CD8(4)^+$ T cell(s); cont, control; #, number.

Figure S2.

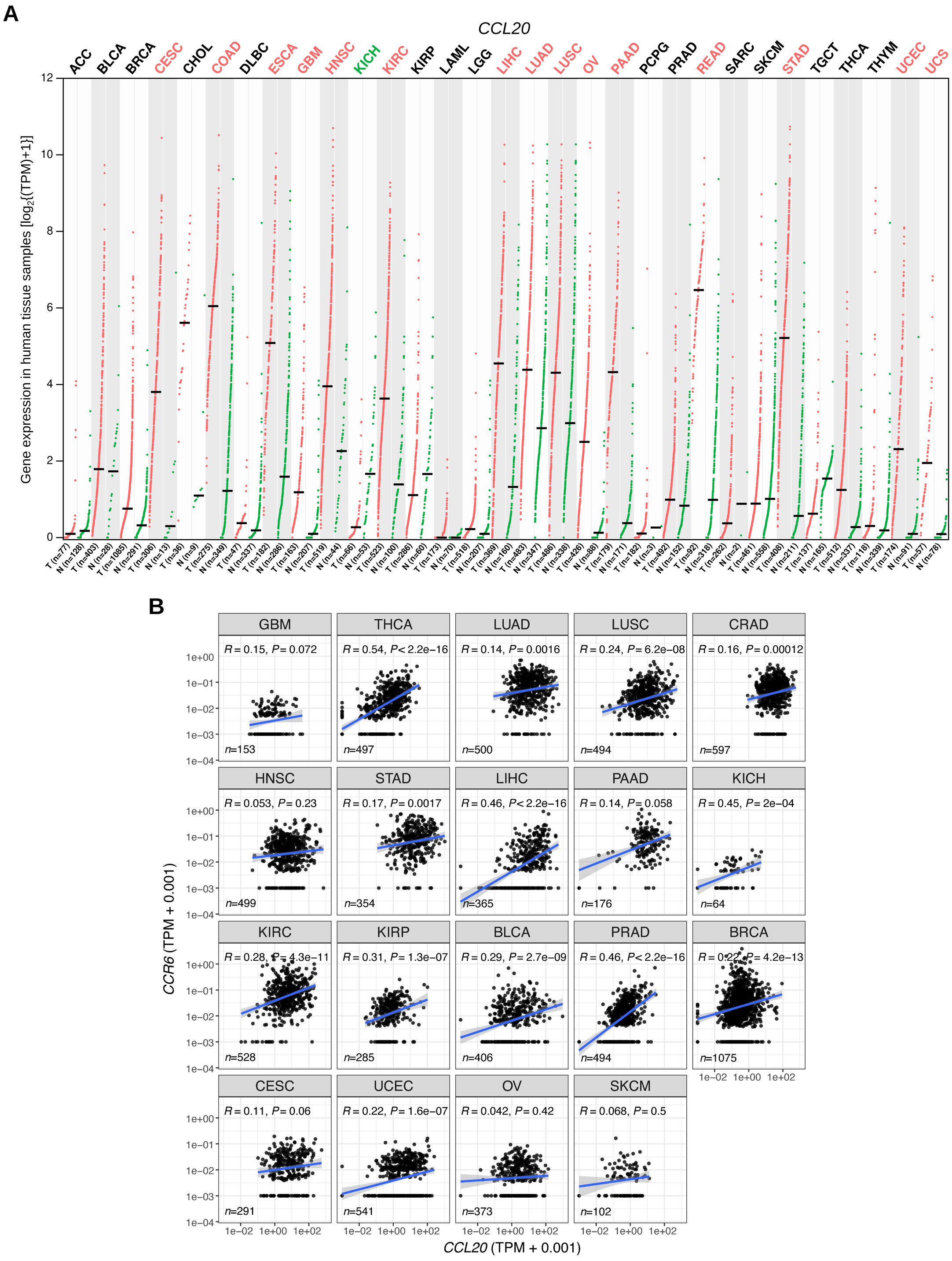
A
CCL20
ACC BLCA BRCA CESC CHOL COAD DLBC ESCA GBM HNSC KICH KIRC KIRP LAML LGG LIHC LUAD LUSC OV PAAD PCPG PRAD READ SARC SKCM STAD TGCT THCA THYM UCEC UCS
Gene expression in human tissue samples [log2(TPM+1)]
0
2
4
6
8
10
12
T (n=77) N (n=128) T (n=403) N (n=28) T (n=1085) N (n=291) T (n=306) N (n=13) T (n=36) N (n=9) T (n=275) N (n=349) T (n=47) N (n=337) T (n=182) N (n=286) T (n=163) N (n=207) T (n=519) N (n=44) T (n=66) N (n=53) T (n=523) N (n=100) T (n=286) N (n=60) T (n=173) N (n=70) T (n=518) N (n=207) T (n=369) N (n=160) T (n=483) N (n=347) T (n=486) N (n=338) T (n=426) N (n=88) T (n=179) N (n=171) T (n=182) N (n=3) T (n=492) N (n=152) T (n=92) N (n=318) T (n=262) N (n=2) T (n=461) N (n=558) T (n=408) N (n=211) T (n=137) N (n=165) T (n=512) N (n=337) T (n=118) N (n=339) T (n=174) N (n=91) T (n=57) N (n=78)
B
GBM R = 0.15, P = 0.072 n=153
THCA R = 0.54, P < 2.2e−16 n=497
LUAD R = 0.14, P = 0.0016 n=500
LUSC R = 0.24, P = 6.2e−08 n=494
CRAD R = 0.16, P = 0.00012 n=597
HNSC R = 0.053, P = 0.23 n=499
STAD R = 0.17, P = 0.0017 n=354
LIHC R = 0.46, P < 2.2e−16 n=365
PAAD R = 0.14, P = 0.058 n=176
KICH R = 0.45, P = 2e−04 n=64
KIRC R = 0.28, P = 4.3e−11 n=528
KIRP R = 0.31, P = 1.3e−07 n=285
BLCA R = 0.29, P = 2.7e−09 n=406
PRAD R = 0.46, P < 2.2e−16 n=494
BRCA R = 0.22, P = 4.2e−13 n=1075
CESC R = 0.11, P = 0.06 n=291
UCEC R = 0.22, P = 1.6e−07 n=541
OV R = 0.042, P = 0.42 n=373
SKCM R = 0.068, P = 0.5 n=102
1e+00
1e−01
1e−02
1e−03
1e−04
1e−02 1e+00 1e+02
CCR6 (TPM + 0.001)
CCL20 (TPM + 0.001)

**Supplementary Figure S2. *CCL20* and *CCR6* gene expressions in human cancers and paired normal tissues.** **A,** *CCL20* expression in 31 types of human tumor tissues (T) as indicated was compared with paired normal tissues (N) using TCGA and the GTEx database obtained from GEPIA. Results are presented as dot plots with median depicted and statistical analysis was performed by four-way ANOVA. Names of cancer types that express the *CCL20* gene higher than paired normal tissue are shown as red. Name of cancer types that expresses the *CCL20* gene lower than paired normal tissue are shown in green. Number (*n*) of samples in every type of tissue is indicated in the panels. **B,** Correlation of *CCL20* and *CCR6* expression in 19 types of human cancers in TCGA. *CCL20* and *CCR6* gene expressions (TPM + 0.001) are plotted on logarithmic scales with linear regression lines and 95% CIs. Number (*n*) of samples, Spearman's Rho (*R*) and unadjusted *P* value are shown in the panels. Abbreviation of cancer types are indicated in Supplementary Table.

Figure S3.

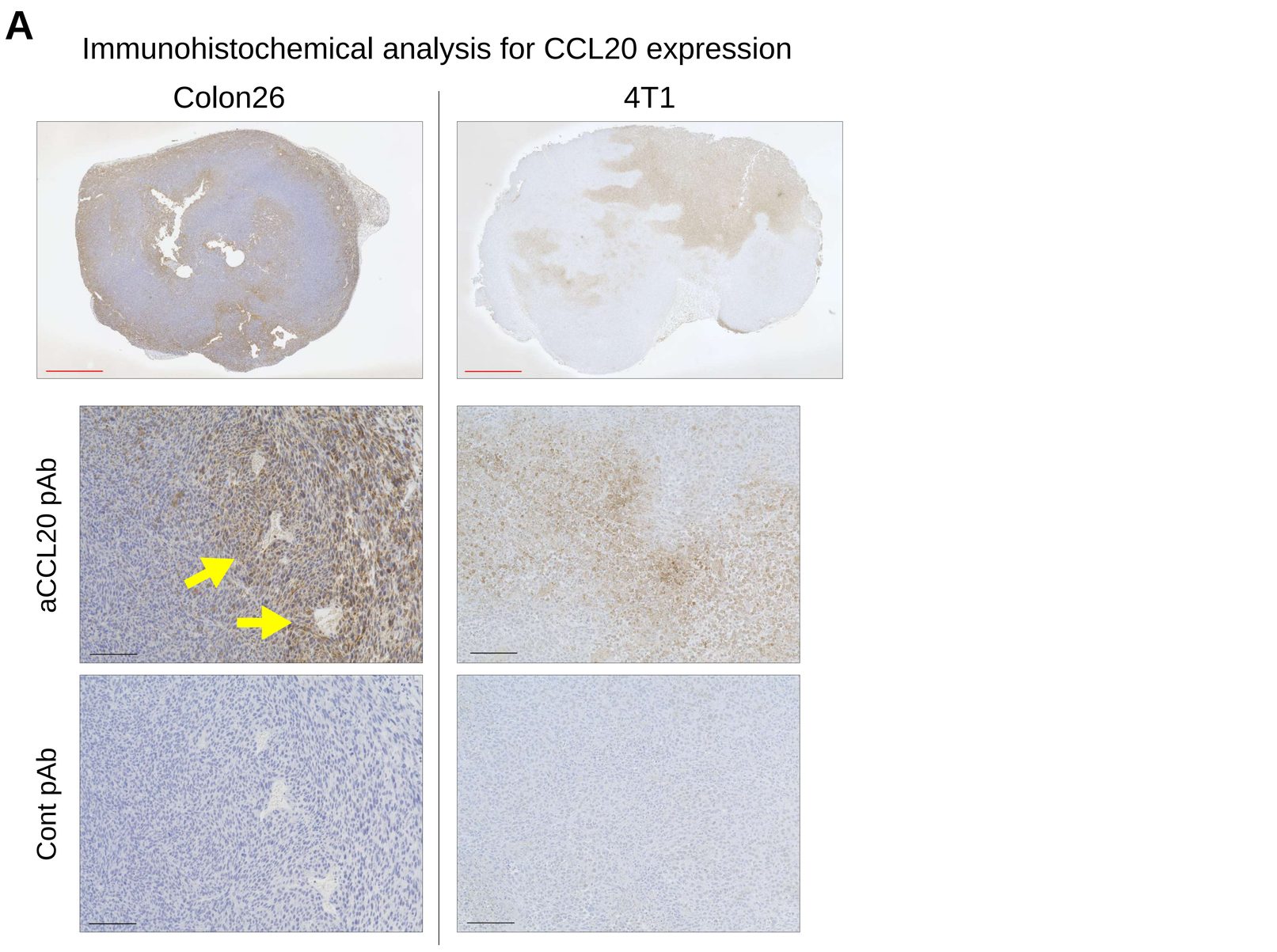
A
Immunohistochemical analysis for CCL20 expression
Colon26
4T1
aCCL20 pAb
Cont pAb

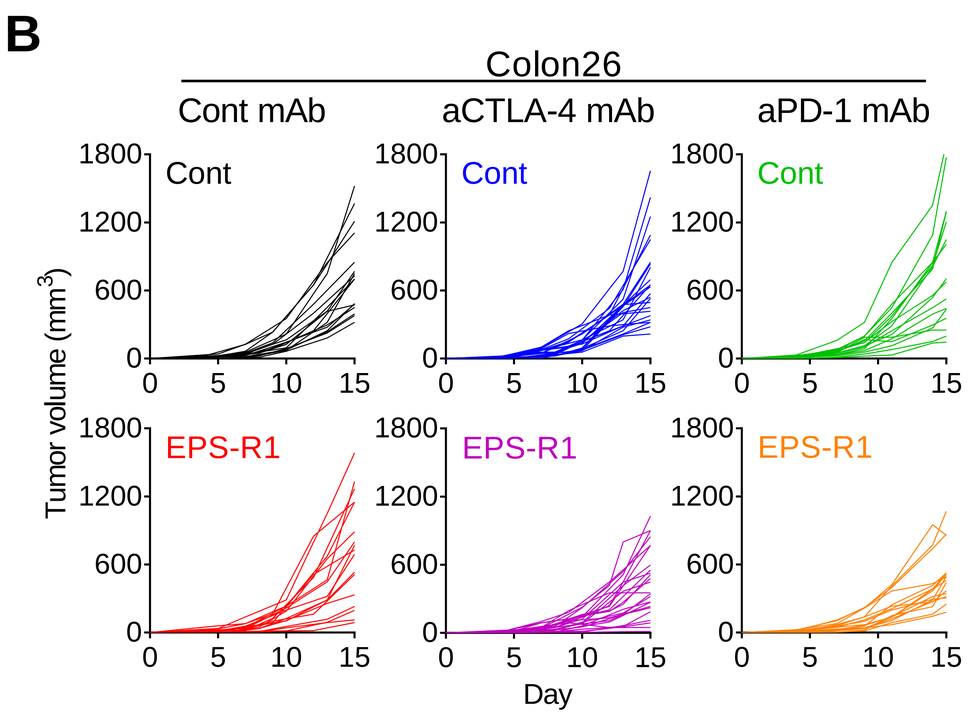
B
Colon26
Cont mAb
aCTLA-4 mAb
aPD-1 mAb
Cont
Cont
Cont
EPS-R1
EPS-R1
EPS-R1
Tumor volume (mm3)
Day

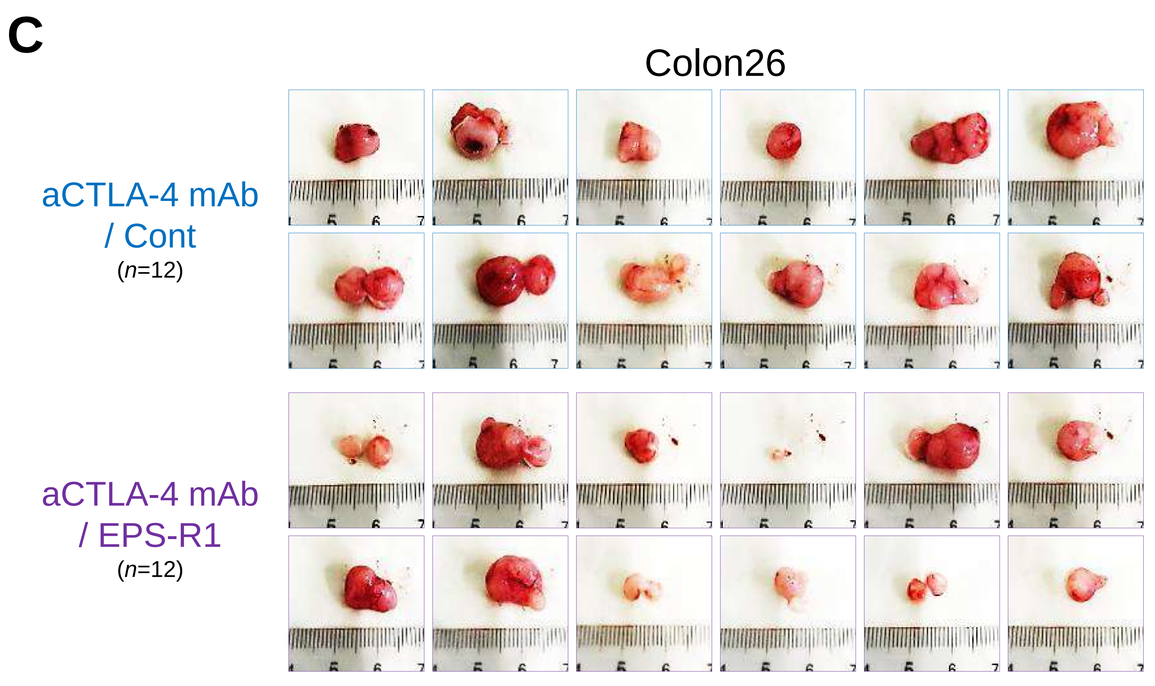
C
Colon26
aCTLA-4 mAb / Cont
(n=12)
aCTLA-4 mAb / EPS-R1
(n=12)

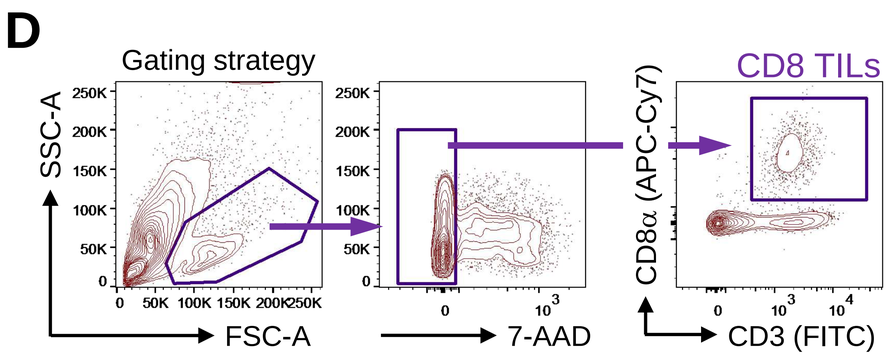
D
Gating strategy
CD8 TILs
SSC-A
FSC-A
7-AAD
CD8α (APC-Cy7)
CD3 (FITC)

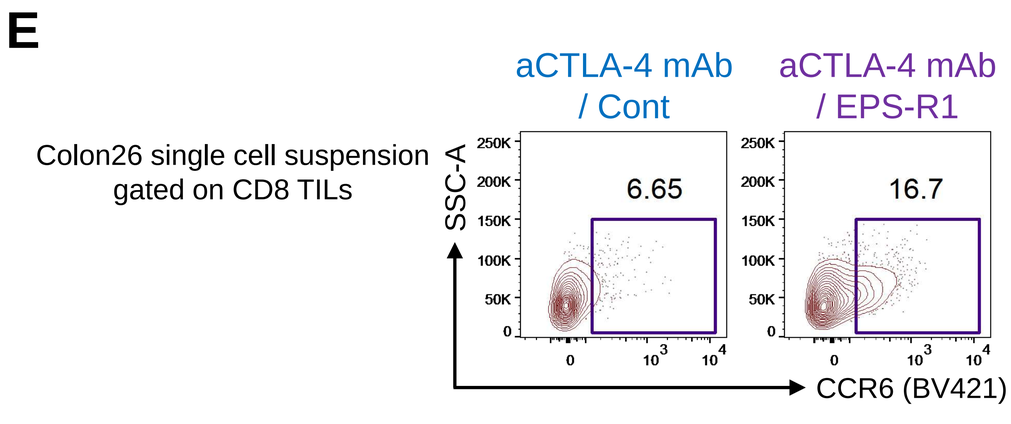
E
Colon26 single cell suspension
gated on CD8 TILs
aCTLA-4 mAb / Cont
aCTLA-4 mAb / EPS-R1
6.65
16.7
SSC-A
CCR6 (BV421)

**Supplementary Figure S3. CCL20 protein expression in Colon26 and 4T1 tumors and anti-tumor effects of ICBs with or without ingestion of EPS-R1 against Colon26 tumors.**
**A,** Immunohistochemical analysis for CCL20 expression of Colon26 and 4T1 tumors growing in BALB/c WT mice on day 15. Mayer's hematoxylin staining was performed as counter staining. Representative macroscopic tissue images (concatenated x40 images) are presented in the top panels and microscopic tissue images (x200) are presented in the middle (stained with anti-CCL20 pAb) and bottom (stained with control immune globulins) panels. Yellow arrows indicate blood vessels. Bar lengths are 1000 μm (in top panels) or 100 μm (in middle and bottom panels) respectively. Similar results were obtained from two independent experiments. **B,** BALB/c WT mice were s.c. inoculated with Colon26 tumor cells and ingestion of EPS-R1 was started on day 0. Some mice were i.p. treated with anti-CTLA-4 mAb or anti-PD-1 mAb on day 4, 7 and 10. Tumor volumes of individual mice (*n*: indicated in Fig. 3C) from three (control and anti-CTLA-4 mAb treatment) or two (anti-PD-1 mAb treatment) independent experiments are presented. **C,** Macroscopic photographs of Colon26 tumors obtained on day 15 from BALB/c WT mice treated with anti-CTLA-4 mAb with or without EPS-R1 in one representative experiment described as in (B) are presented with the ruler scale (mm). **D,** Single cell suspensions were prepared from Colon26 tumors treated with anti-CTLA-4 mAb with or without EPS-R1 ingestion, and CCR6 expression on $CD8^+$ T cells was then analyzed using the indicated gate setting process by flow cytometry. **E,** Representative contour plots of CCR6 expression on $CD8^+$ T cells infiltrating in Colon26 tumors treated with anti-CTLA-4 mAb or anti-CTLA-4 mAb/EPS-R1 are demonstrated with % of gated $CCR6^+$ cells. Square gates were set basing on the staining profile with isotype-matched control mAb.
aCCL20(CTLA-4, PD-1), anti-CCL20(CTLA-4, PD-1); cont, control; FSC-A, forward scatter area; SSC-A, side scatter area; CD8 TILs, $CD8^+$ TILs.

Figure S4.

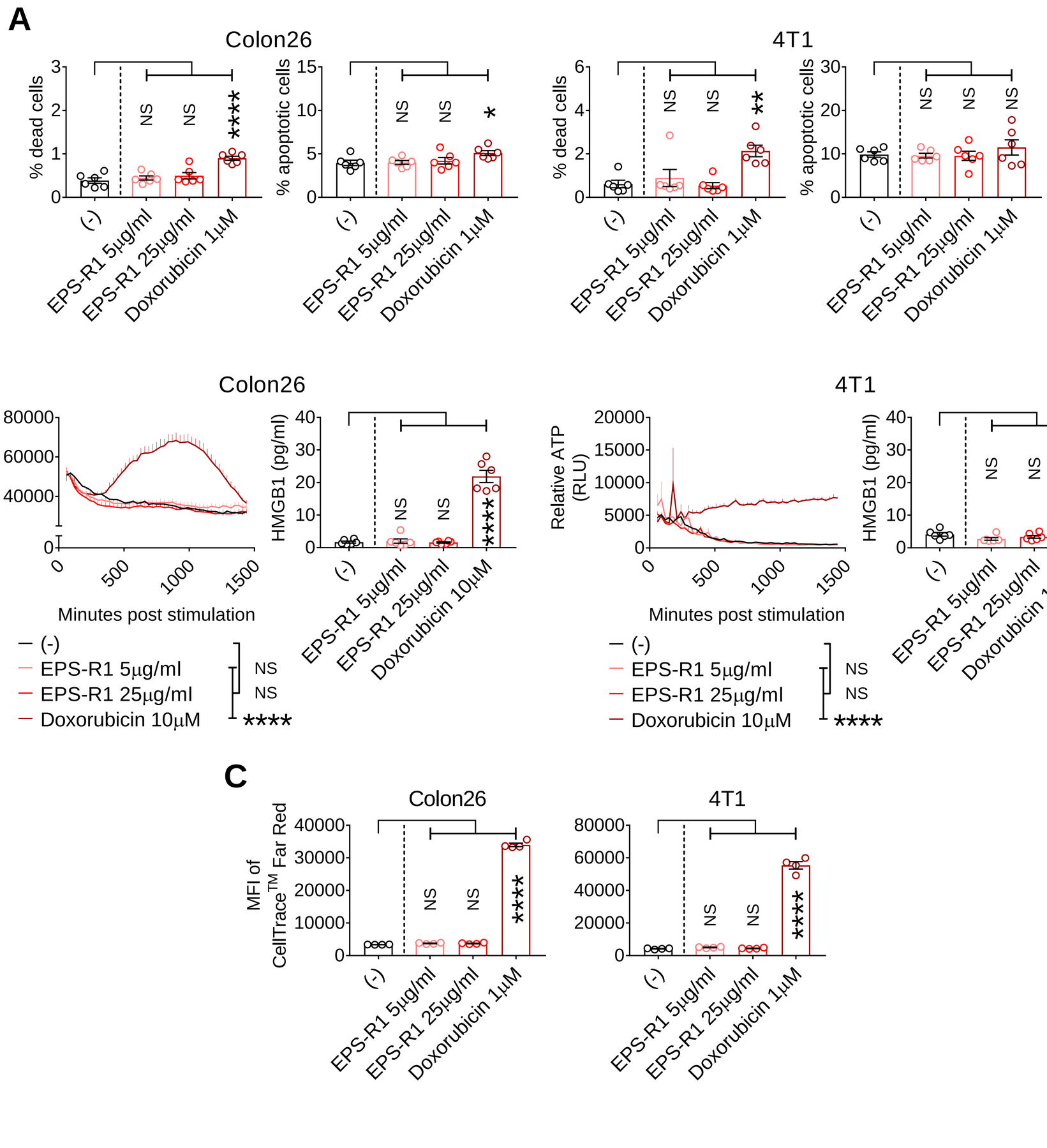


**Supplementary Figure S4. Effect of EPS-R1 on Colon26 or 4T1 tumor cells *in vitro*.**
**A - C,** Colon26 or 4T1 tumor cells were co-cultured with EPS-R1 or doxorubicin (concentration: indicated in each panel) as described below. % dead cells (7-AAD$^{high}$ annexin V$^{high}$) and apoptotic cells (7-AAD$^{-\text{ to low}}$ annexin V$^{low}$) were analyzed after 24 h co-culture using flow cytometry ($n$ = 6) (**A**). The relative amount of secretory ATP was periodically detected as luminescence of luciferase for every 30 minutes from 1 to 24 h after co-culture ($n$ = 4), and secretory HMGB1 was detected by ELISA after 24 h co-culture ($n$ = 6) (**B**). To analyze cell proliferation, mean fluorescent intensity (MFI) of CellTrace™ Far Red was examined after 4 days co-culture using flow cytometry ($n$ = 4) (**C**). Results are presented as dot plots with mean ± SEM (A, B in HMGB1, and C) or mean ± SEM with connected line (B in ATP). Statistical analyses were performed by one-way ANOVA with Dunnett correction (A, B in HMGB1, and C) or two-way ANOVA with Dunnett correction (B in ATP). NS, not significant. *$P$ < 0.05, **$P$ < 0.01, ****$P$ < 0.0001. Similar results were obtained from three independent experiments (A - C).
RLU, relative light unit.

# Figure S5.

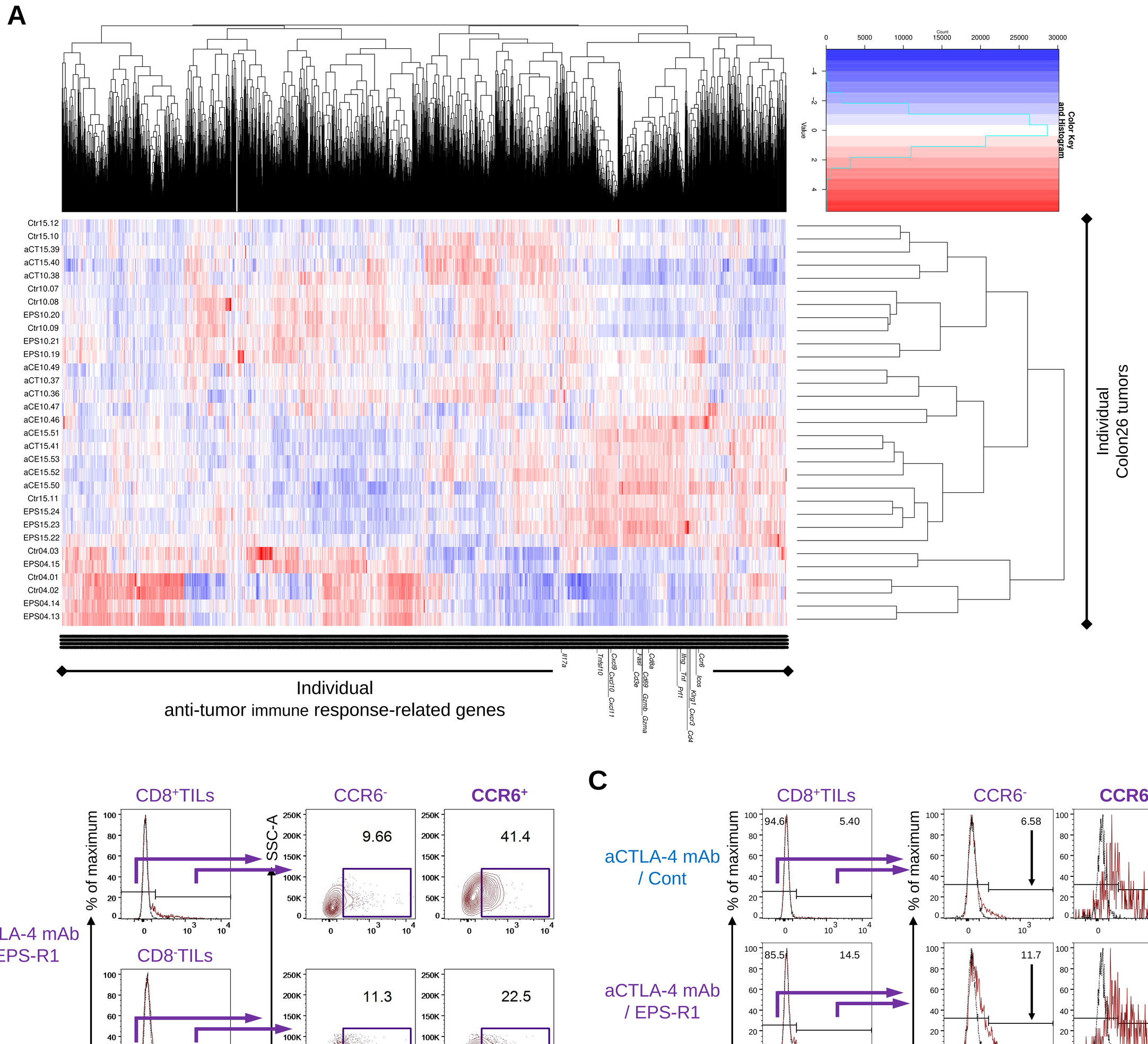


Colon26 CD45+ single cell suspension
gated on indicated TILs (**B**-**D**)

**Supplementary Figure S5. Heat map and dendrogram of immune-related gene expression demonstrated by RNAseq analysis and IFN-γ/granzyme B expression amongst CXCR3/CCR6-expressing $CD8^+$ T cells infiltrating into anti-CTLA-4 mAb-treated tumors.**

**A,** BALB/c WT mice were s.c. inoculated with Colon26 tumor cells and some mice were i.p. treated with anti-CTLA-4 mAb and/or dietary EPS-R1. RNA samples were prepared from Colon26 tumor masses on day 4, 10 and 15 (*n* = 3 or 4 each group), and RNAseq analysis was then performed as described in the METHODS. Heat map of rows and columns (each gene expression was processed by *z*-score normalization) are clustered. All analyzed genes in Fig. 4C are indicated. Ctr: control, aCT: anti-CTLA-4 mAb-treated, EPS: EPS-R1-treated, aCE: anti-CTLA-4 mAb/EPS-R1-treated (e.g.; aCE10.48 = anti-CTLA-4 mAb/EPS-R1-treated tumor on day 10: sample number 48). **B,** $CD45^+$ cells were isolated from single cell suspensions prepared from Colon26 tumors treated with anti-CTLA-4 mAb with EPS-R1 ingestion on day 15. CCR6 and IFN-γ expression of $CD8^+$ or $CD8^-$ TILs were then analyzed by flow cytometry. Representative histograms of CCR6 expression on $CD8^+$ or $CD8^-$ TILs and representative contour plots of IFN-γ expression in $CCR6^{+ \text{ or } -}$ $CD8^+$ or $CCR6^{+ \text{ or } -}$ $CD8^-$ TILs are presented. Square gates were set basing on the staining profile with isotype-matched control mAb. Staining profiles with isotype-matched control mAb are shown as dotted black lines in all the histograms. **C,** $CD45^+$ cells were isolated from single cell suspensions prepared from Colon26 tumors treated with anti-CTLA-4 mAb with or without EPS-R1 ingestion on day 15. CCR6 and CXCR3 expression on $CD8^+$ TILs were then analyzed by flow cytometry. Representative histograms of CXCR3 expression on $CCR6^+$ or $CCR6^-$ $CD8^+$ TILs are demonstrated. Staining profiles with isotype-matched control mAb are shown as dotted black lines in all the histograms. **D,** $CD45^+$ cells were isolated from single cell suspensions prepared from Colon26 tumors treated with anti-CTLA-4 mAb with or without EPS-R1 ingestion on day 15. CCR6, CXCR3, IFN-γ and granzyme B expression on $CD8^+$ TILs were then analyzed by flow cytometry. Representative contour plots of IFN-γ and granzyme B expression in CXCR3/$CCR6^+$ or CXCR3/$CCR6^-$ $CD8^+$ TILs are demonstrated. Quadra gate were set basing on the staining profile with isotype-matched control mAb. **E,** The percentage of IFN-γ/granzyme B expressing populations amongst CXCR3/CCR6-expressing $CD8^+$ T cells presented in (B - D) are demonstrated as bar and circle graphs following gate settings.

aCTLA-4, anti-CTLA-4; SSC-A, side scatter area; cont, control.

# Figure S6.

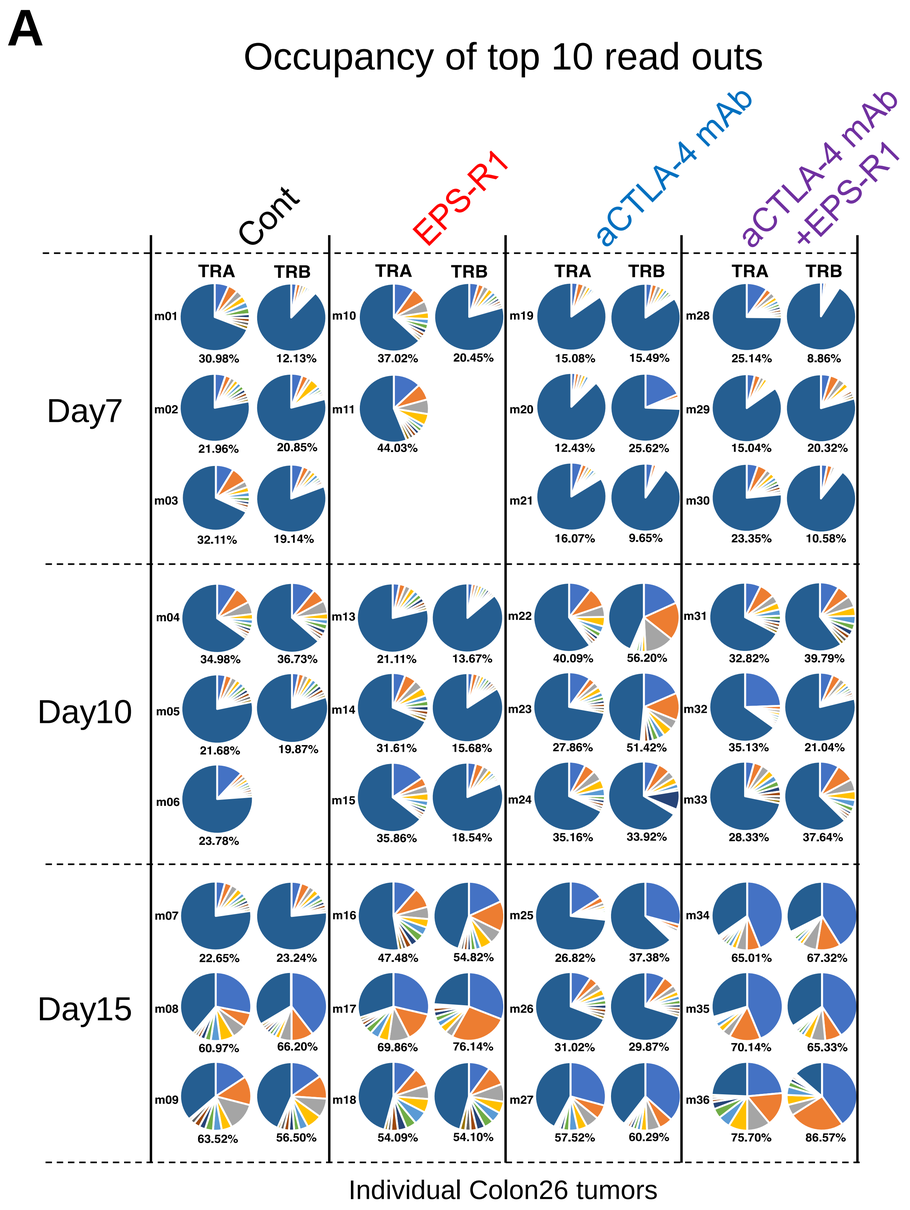
A
Occupancy of top 10 read outs
Cont
EPS-R1
aCTLA-4 mAb
aCTLA-4 mAb +EPS-R1
TRA
TRB
Day7
Day10
Day15
m01 30.98% 12.13%
m02 21.96% 20.85%
m03 32.11% 19.14%
m10 37.02% 20.45%
m11 44.03%
m19 15.08% 15.49%
m20 12.43% 25.62%
m21 16.07% 9.65%
m28 25.14% 8.86%
m29 15.04% 20.32%
m30 23.35% 10.58%
m04 34.98% 36.73%
m05 21.68% 19.87%
m06 23.78%
m13 21.11% 13.67%
m14 31.61% 15.68%
m15 35.86% 18.54%
m22 40.09% 56.20%
m23 27.86% 51.42%
m24 35.16% 33.92%
m31 32.82% 39.79%
m32 35.13% 21.04%
m33 28.33% 37.64%
m07 22.65% 23.24%
m08 60.97% 66.20%
m09 63.52% 56.50%
m16 47.48% 54.82%
m17 69.86% 76.14%
m18 54.09% 54.10%
m25 26.82% 37.38%
m26 31.02% 29.87%
m27 57.52% 60.29%
m34 65.01% 67.32%
m35 70.14% 65.33%
m36 75.70% 86.57%
Individual Colon26 tumors

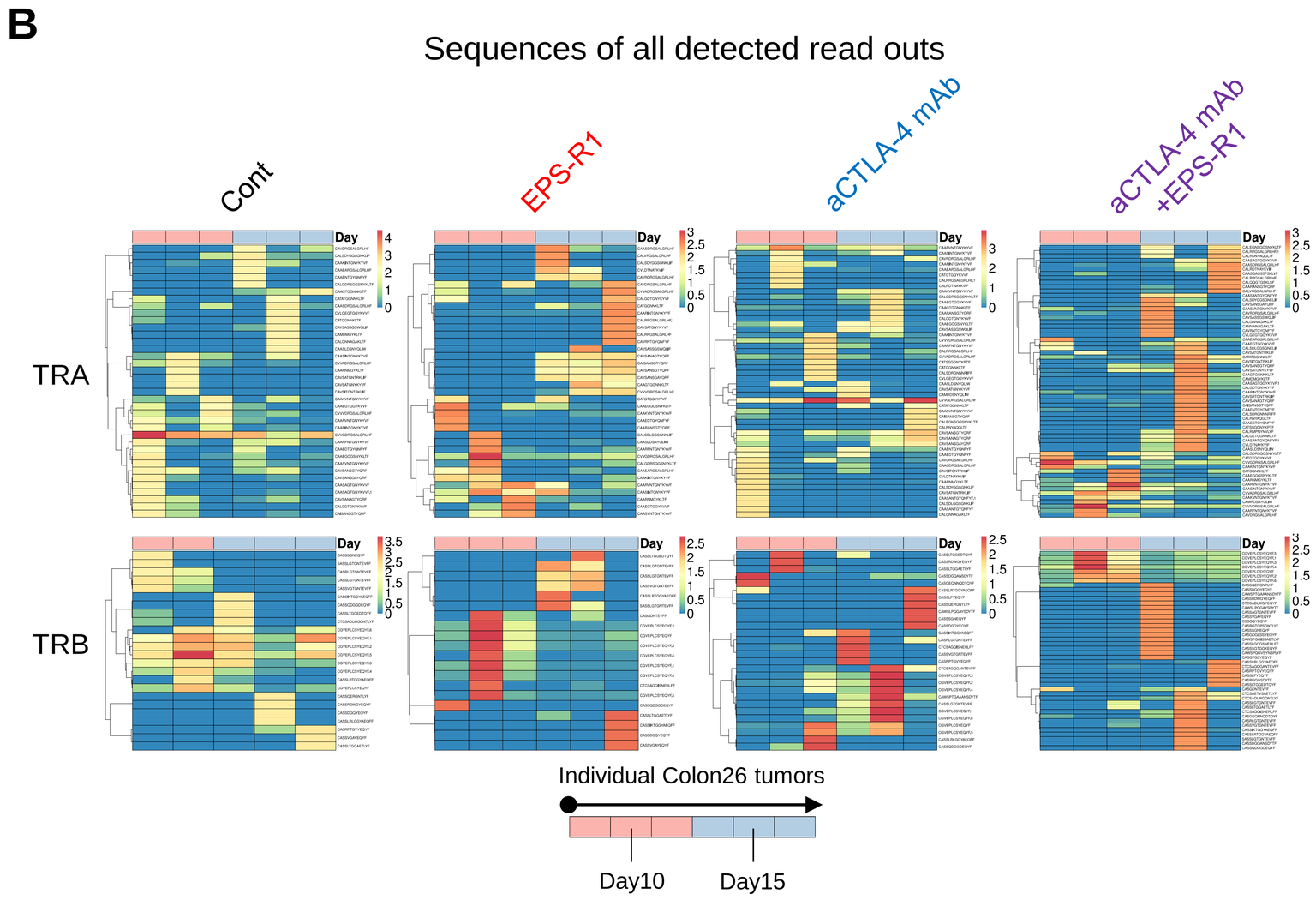
B
Sequences of all detected read outs
Cont
EPS-R1
aCTLA-4 mAb
aCTLA-4 mAb +EPS-R1
TRA
TRB
Day
Individual Colon26 tumors
Day10
Day15

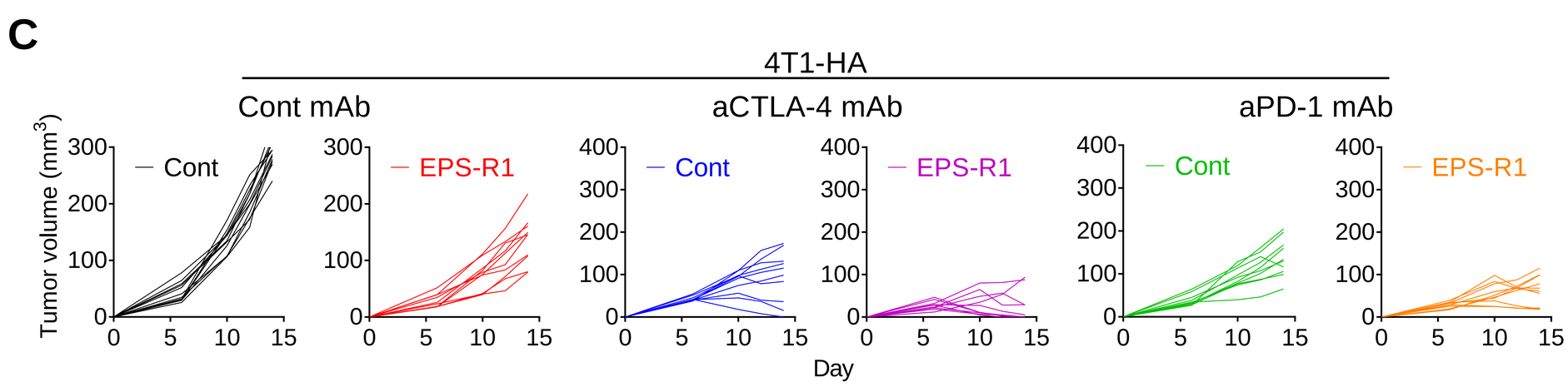
C
4T1-HA
Cont mAb
aCTLA-4 mAb
aPD-1 mAb
Tumor volume (mm3)
Cont
EPS-R1
Day

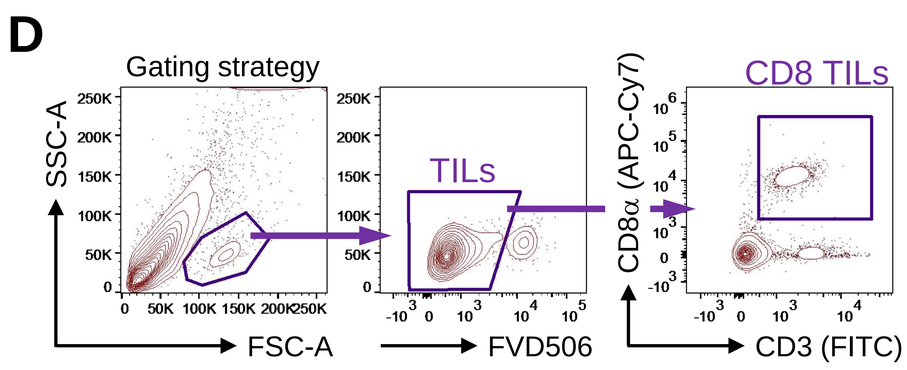
D
Gating strategy
SSC-A
FSC-A
TILs
FVD506
CD8 TILs
CD8α (APC-Cy7)
CD3 (FITC)

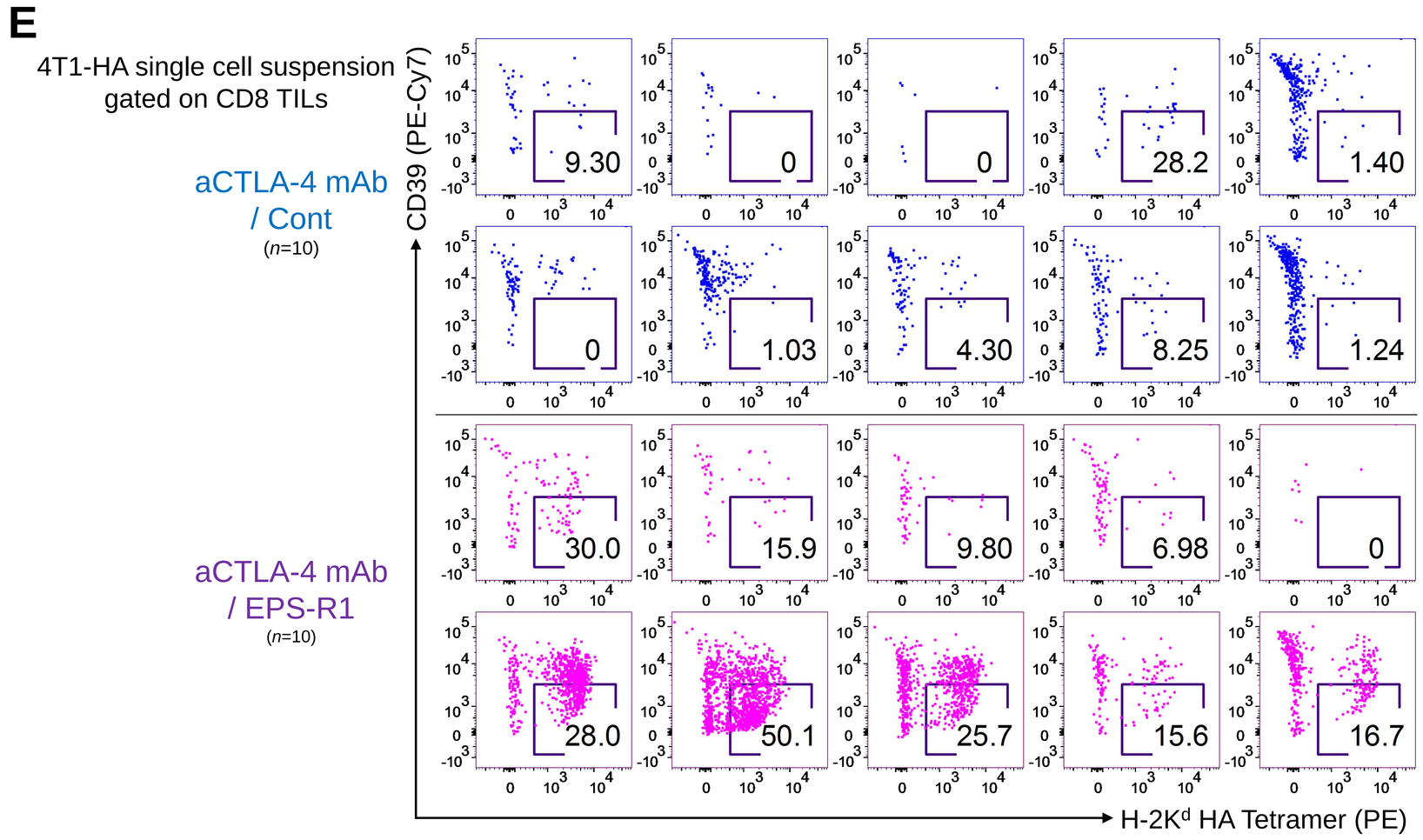
E
4T1-HA single cell suspension gated on CD8 TILs
aCTLA-4 mAb / Cont
(n=10)
aCTLA-4 mAb / EPS-R1
(n=10)
CD39 (PE-Cy7)
H-2Kd HA Tetramer (PE)
9.30
0
0
28.2
1.40
0
1.03
4.30
8.25
1.24
30.0
15.9
9.80
6.98
0
28.0
50.1
25.7
15.6
16.7

**Supplementary Figure S6. TRA and TRB sequences detected in Colon26 tumors and anti-tumor effects of anti-CTLA-4 mAb with or without ingestion of EPS-R1 against 4T1-HA tumors.**
**A,** BALB/c WT mice were s.c. inoculated with Colon26 tumor cells and treated with dietary EPS-R1 and/or anti-CTLA-4 mAb. RNA samples were prepared from tumors (*n* = 2 - 3 each group) on day 7, 10 and 15. TCR genes were then analyzed by deep sequencing on individual samples. Occupancy of top 10 read outs in total TCR sequences in individual tumors is presented in a pie chart, and occupancy (%) of top 10 sequences is demonstrated below every panel. Results of one of TRB sequence in control on day 10 (m06) and in EPS-R1 on day 7 (m11) were not obtained due to poor RNA conditions. **B,** All detected TRA and TRB sequences both on day 10 and day 15 in the experiments described in (A) are presented as a heat map. **C,** BALB/c WT mice were s.c. inoculated with 4T1-HA tumor cells and ingestion of EPS-R1 was started on day 0. Some mice were i.p. treated with anti-CTLA-4 mAb or anti-PD-1 mAb on day 4, 7 and 15. Tumor volumes of individual mice from one representative experiment are presented. **D,** Gate setting process for live $CD8^+$ T cells in single cell suspensions prepared from 4T1-HA tumors. **E,** Dot plots profiles of CD39 and HA-specific TCR expression on $CD8^+$ TILs in 4T1-HA tumors treated with anti-CTLA-4 mAb with or without EPS-R1 ingestion on day 15. All results of individual mice in one representative experiment were presented. Square gates were set on $CD39^{low}$ HA-specific $TCR^+$ cells basing on the staining profile with isotype-matched control mAb and control tetramer, and % of gated cells in $CD8^+$ T cells are shown in every panel.
cont, control; aCTLA-4(PD-1), anti-CTLA-4(PD-1); FSC-A, forward scatter area; SSC-A, side scatter area; CD8 TILs, $CD8^+$ TILs.

Figure S7.

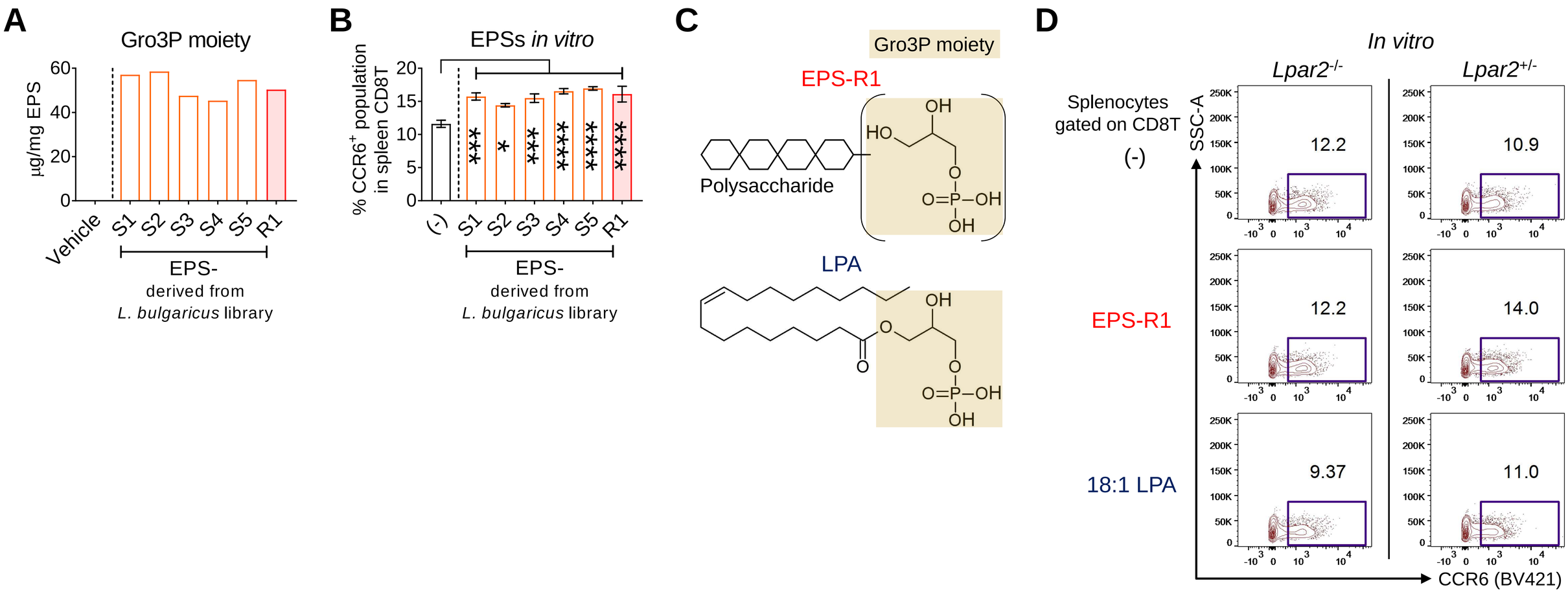


**Supplementary Figure S7. CCR6 expression on CD8⁺ T cells when stimulated with Gro3P-containing EPSs *in vitro* and representative contour plots of CCR6 expression on splenic CD8⁺ T cells of ICR *Lpar2*$^{-/-}$ or *Lpar2*$^{+/-}$ mice when stimulated with EPS-R1 or 18:1 LPA *in vitro*.**

**A,** EPSs that contain the Gro3P structure were prepared from skim milk fermented with other different strains (EPS-S1~S5) of *L. bulgaricus* as the EPS-R1 preparation (See METHODS). Contents of Gro3P in EPSs examined by LC-MS/MS are presented as μg/mg. **B,** Splenocytes were prepared from BALB/c WT mice and stimulated with EPS-S1~S5 or EPS-R1, respectively, for 24 h *in vitro*. CCR6⁺ population amongst CD8⁺ T cells was then examined by flow cytometry ($n$ = 8). Results are presented as mean ± SEM. Statistical analysis was performed by one-way ANOVA with Dunnett correction. NS, not significant. *$P$ < 0.05, ***$P$ < 0.001, ****$P$ < 0.0001. **C,** Schematic structural formulae of EPS-R1 and LPA. **D,** Representative contour plots of CCR6 expression on splenic CD8⁺ T cells of ICR *Lpar2*$^{-/-}$ or *Lpar2*$^{+/-}$ mice when stimulated with EPS-R1 or 18:1 LPA. Percentage of gated CCR6⁺ cells are presented in the panels. Square gates were set basing on the staining profile with isotype-matched control mAb. Similar results were obtained from three independent experiments (A and B).

CD8T, CD8⁺ T cell(s); SSC-A, side scatter area.

Figure S8.

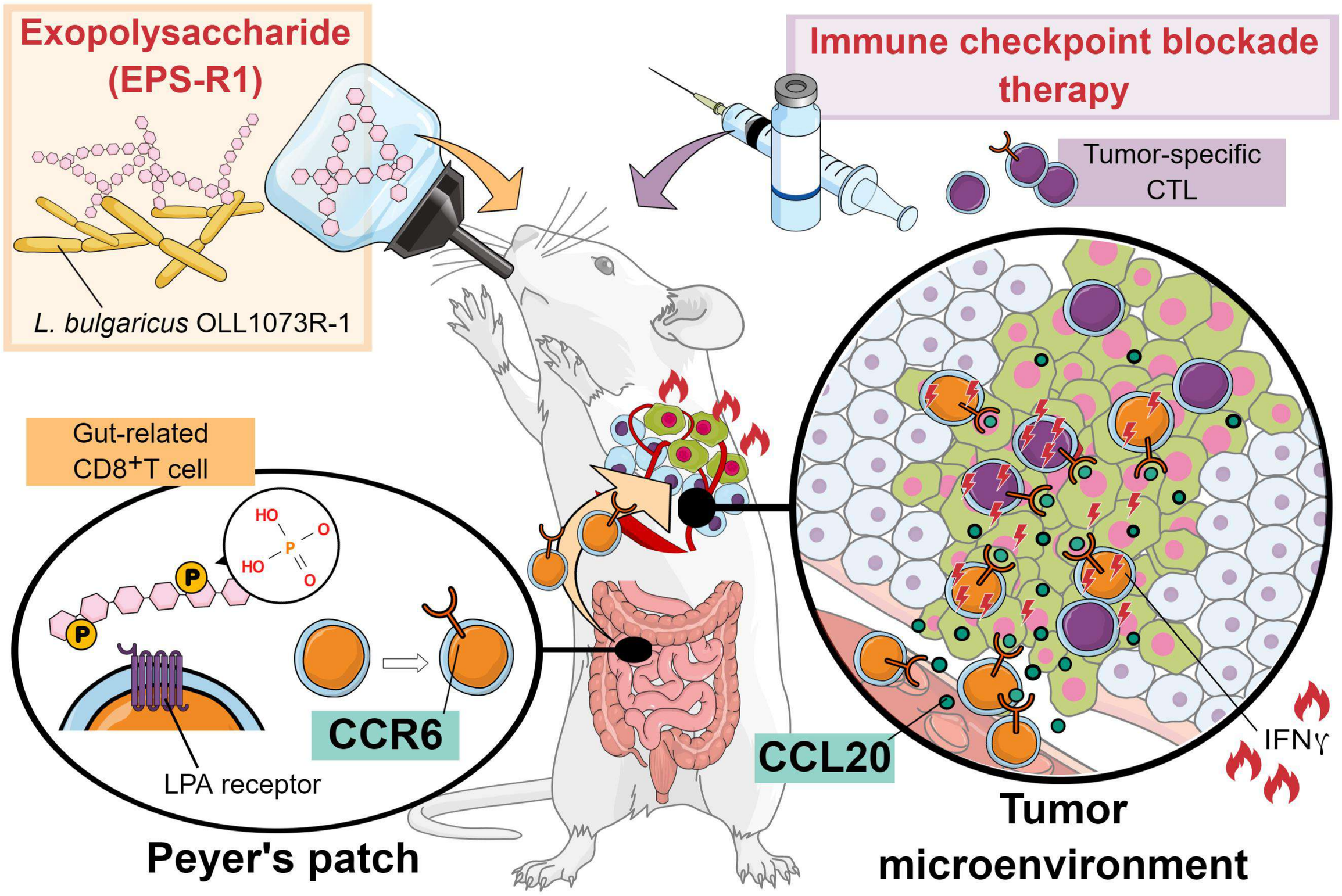


**Supplementary Figure S8. Graphical abstract showing the possible mechanism that dietary EPS-R1 ingestion augments the therapeutic effects of ICBs in a tumor-bearing mouse.**

Figure S9.

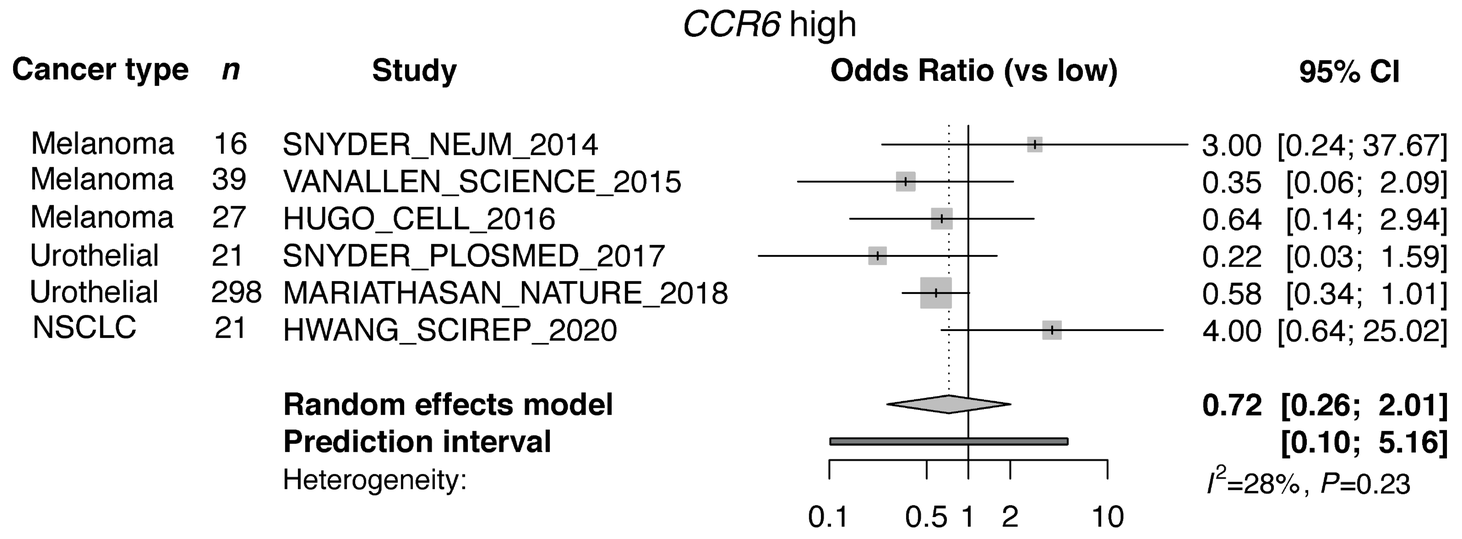


**Supplementary Figure S9. Correlation between *CCR6* expression and response to ICB therapies.**
Forest plot of studies with ICB response and *CCR6* expression. The analysis included publicly available study cohorts providing both gene expression data and ICB treatment response data. Odds ratios with 95% CIs on a logarithmic scale are plotted. Size of the square marks indicates the number of patients. Pooled effect size and the associated 95% CIs are described in a diamond. The 95% prediction interval of the pooled effect is described in a horizontal bar. Between-study heterogeneity variance ($I^2$ value) and number ($n$) of samples are shown in the panel. Abbreviation of cancer types are indicated in Supplementary Table.

Figure S10.

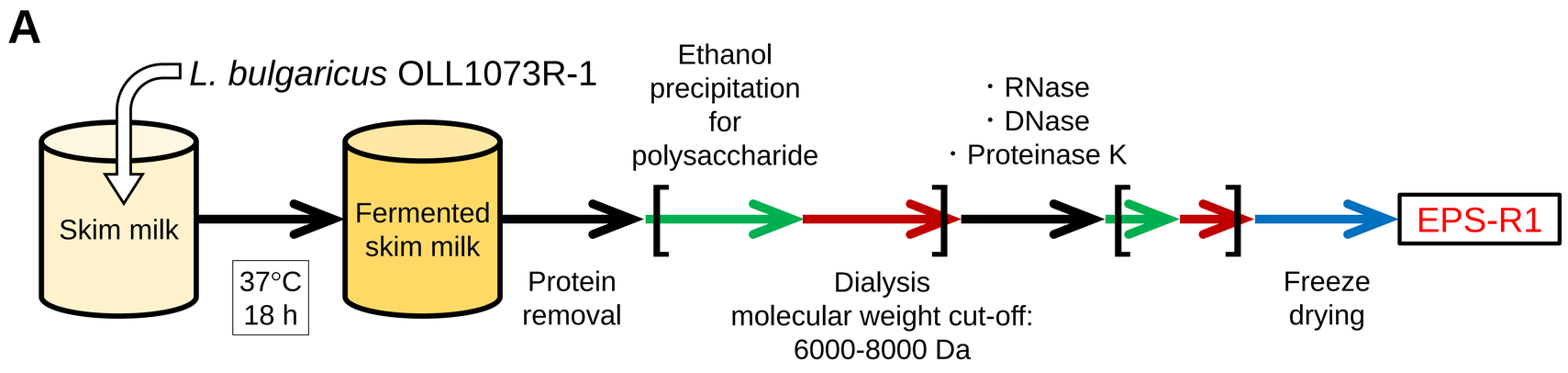


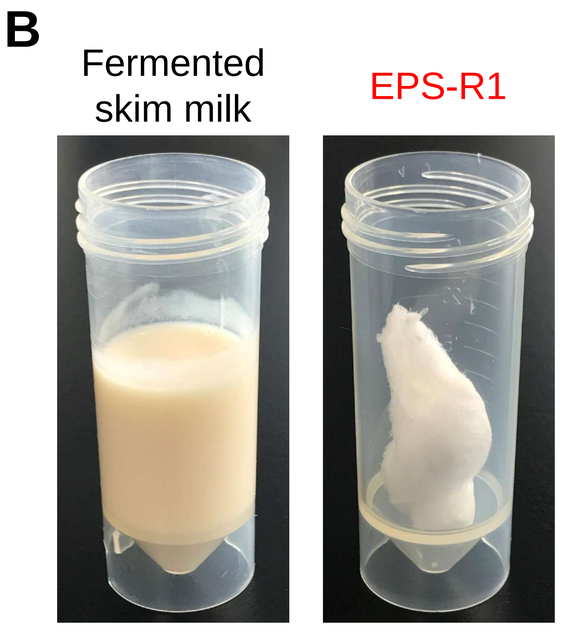


**Supplementary Figure S10. EPS-R1 preparation protocol.**
**A,** Flow chart of EPS-R1 preparation from skim milk fermented with *L. bulgaricus* OLL1073R-1. **B,** Macroscopic photographs of fermented skim milk and EPS-R1.